

# **VALIDATION OF CATHARE TH-SYS CODE AGAINST EXPERIMENTAL REFLOOD TESTS**

**S. Lutsanych, F. Moretti and F. D'Auria**

University of Pisa, San Piero a Grado Nuclear Research Group

Via Livornese 1291, 56122, San Piero a Grado, Pisa, Italy

s.lutsanych@ing.unipi.it; f.moretti@ing.unipi.it; f.dauria@ing.unipi.it

## **ABSTRACT**

This paper presents results of a code validation activity that has been carried out at the University of Pisa within the EC-funded NURESAFE project, aimed to assess CATHARE2 v2.5\_3 Mod3.1 code capabilities to simulate scenarios featuring reflood conditions. For such purpose, experimental data available from FEBA and ACHILLES separate-effect test facilities was used.

In order to set-up a reference calculation model, rigorous sensitivity studies have been performed for every of the selected experimental test facilities. Quantitative analysis of the results has been carried out for all of the considered tests, using the Fast Fourier Transform Based Method (FFTB) for accuracy quantification of code predictions.

The calculations of experimental tests of ACHILLES facility have been performed with CATHARE2 v2.5\_3 mod 3.1 using both 1-D and 3-D models. The no-regression of the results predicted by such code was successfully checked through qualitative and quantitative comparison with results obtained by the one of previous code versions: CATHARE2 v2.5\_2 mod 7.1.

An assessment of the capabilities of the new CATHARE3 v1.3.13 code to simulate reflood phenomena using both two- and three-field 1-D models has then been carried out, based on the same ACHILLES tests. Simulations by CATHARE3 (three-field) exhibit faster quenching than CATHARE2, mainly due to the presence of the droplet field enhancing the heat exchange from the fuel rod simulators.

The performed qualitative analysis has shown the ability of CATHARE2 code to capture the main features of the reflood phenomena using appropriate modeling. Nonetheless, the quantitative analysis shows a systematic underprediction of the PCT and faster quenching in the majority of tests.

## **KEYWORDS**

CATHARE, REFLOODING, MULTI-FIELD, VALIDATION, ACCURACY

## **1. INTRODUCTION**

The rewetting characteristics of the overheated core after the Loss Of Coolant Accident (LOCA) was one of the most interesting research topics in 70's and still has a significant influence on acceptance criteria in licensing and probabilistic safety analyses. Large break scenarios involve a very rapid depressurization with significant emptying of the primary system and core uncovering.

When the primary system pressure falls below the injection pressure of the various Emergency Core Cooling Systems (ECCS), borated coolant enters the primary system and flows through the available paths to refill the lower-plenum and then to reflood and finally recover the core.

The CATHARE developing strategy comprises qualification process, which is based on: Code Verification, Validation procedure on separate-effect and integral test facilities. Experimental data covering a wide range of operation parameters during reflood phase is available from FEBA and ACHILLES separate-effect test facilities and is an excellent exercise for CATHARE code qualification, based on peak cladding temperature (PCT) and quench front motion predictions on the level of fuel assemblies with a typical Pressurized Water Reactor (PWR) power and fluid conditions.

In current work, different models of FEBA and ACHILLES experimental test bundle have been developed using CATHARE2 and CATHARE3. The capability of codes to represent complex phenomena during reflood at different experimental conditions has been assessed, comparison of the results with measured data has been carried out and accuracy of code predictions was quantified.

## 2. CATHARE2 AND CATHARE3 CODES GENERAL OVERVIEW

CATHARE2 [1] was developed in Grenoble by the Commissariat à l'Energie Atomique (CEA), Electricité de France (EDF), AREVA and Institut de Radioprotection et de Sûreté Nucléaire (IRSN) to perform best-estimate calculations of pressurized water reactor accidents. It is based on a two-fluid six-equation model with a unique set of constitutive laws. Various modules offer space discretization adapted to volumes (0-D), pipes (1-D) or vessels (3-D) ready to assemble for any reactor design or test facility. The discretization of all terms of the equations is fully implicit in 1-D and 0-D modules and semi-implicit in 3-D elements including inter-phase exchange, pressure and convection terms, and the resulting nonlinear equations are solved using classical Newton-Raphson iterative method.

CATHARE3 [2] is an advanced system code developed by CEA within the NEPTUNE multiscale thermal-hydraulic platform [3]. In addition to the two-fluid, 6-equation model already used in CATHARE2, a new three-field model has been implemented in CATHARE3, including a liquid droplet field, a continuous liquid field and a gas field. This advanced model has been developed in order to improve the flow simulation when liquid droplets and continuous liquid flow are at significantly different velocities. Specific closure relations are implemented in CATHARE3 to describe a droplet field: droplet entrainment flux, droplet deposition flux, interfacial friction for droplets, heat transfer between droplets and wall and heat transfer between droplets and gas field, droplet diameter correlations and flow regime transitions. The numerical calculation scheme used by CATHARE3 is similar to the one employed in the CATHARE2 code [4]. The set of conservation equations and closure relations is discretized using a finite difference scheme with staggered spatial meshings and the donor-cell method.

## 3. VALIDATION OF CATHARE AGAINST FEBA REFLOODING EXPERIMENTS

### 3.1. Description of FEBA test facility

The FEBA (Flooding Experiments with Blocked Array) program has been performed at KfK Karlsruhe, Germany [5]. This Separate-Effect Test Facility (SETF) was designed for the reflooding tests with possibility of maintaining constant flooding rates and constant back pressure. The test section consists of a full-length 5 x 5 rod bundle of PWR fuel rod dimensions (Fig. 1) utilizing electrically heated rods (Nichrome wire and cladding with magnesium oxide insulator inside) with a cosine power profile. The rod bundle is placed in housing made of stainless steel and insulated to reduce heat losses to environment.

### 3.2. Modeling of FEBA with CATHARE2

The FEBA test assembly has been modelled by CATHARE2 V2.5\_3 mod 3.1 code by one single 1-D component representing the core bundle (heated part, 3900 mm) with only 1 heat rod element, inlet and outlet boundary conditions (Fig. 2). The 1-D component is composed of 39 vertical meshes in the core (length of 1 mesh is 0.1 m). The thick-wall housing is modelled (thickness is 6.5 mm), whereas unheated part of rods, lower and upper plenum are not modelled. The CATHARE reflow correlations (REFLCHAR) are used for both the heater rods to fluid and housing to fluid heat transfers.

Spacer grids have been taken into account during the nodalization set-up and the proper  $K_{loss}$  coefficients have been allocated at corresponding junctions in order to simulate the pressure loss due to flow restriction. No flow area reduction or change in hydraulic diameter has been modeled at locations of the spacer grids. The main model properties are summarized in Table 1. It should be also noted that the reference model has been developed using the available description of FEBA facility and experimental measurements of test 216. However, no special tuning has been applied to get the best possible agreement with experimental data, i.e. the so-called “best practice” has been used during the model development.

The heat-up conditioning phase has been simulated in order to reach the Start of Transient (SoT) conditions. The experimental level of power was not given, its value is tuned so to have correct initial values of the temperature of the housing ( $635^{\circ}\text{C}$  at 1625 mm) and of the cladding temperature ( $800^{\circ}\text{C}$  at 1680 mm). The power of the test bundle during this step is set to 6.0% of the nominal power of FEBA test 216 (i.e.  $6.0\% * 200 \text{ KW} = 12\text{KW}$ ).

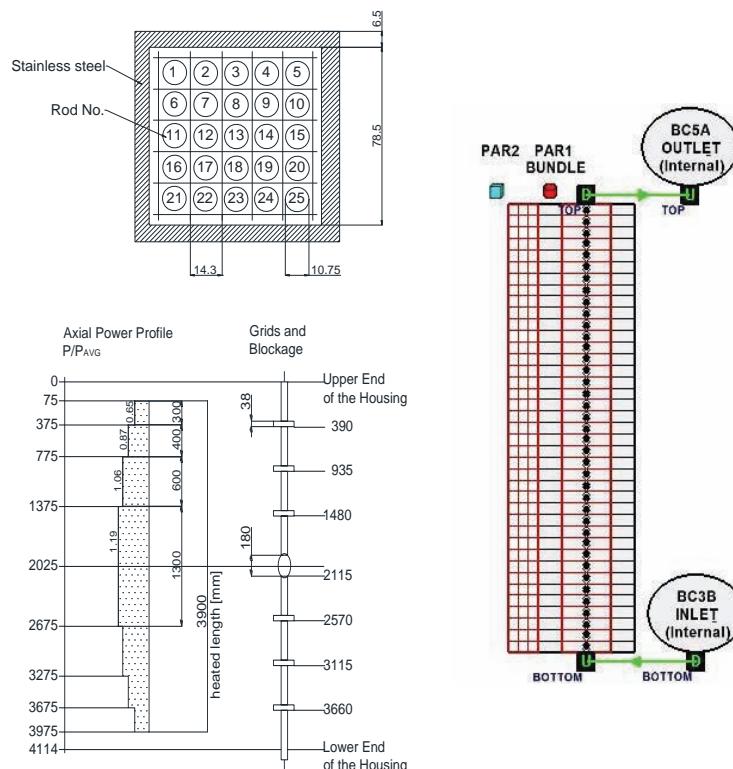


**Figure 1. FEBA rod bundle – cross-section view and axial power profile distribution.**

**Table 1. Summary of CATHARE2 model of FEBA facility**

| Parameter   | Value                             |
|---|-----------------------------------|
| Total height/length                                 | 4.322 m                           |
| Length of the heated part                           | 3.9 m                             |
| Nodes in heated part                                | 39                                |
| Flow area   | $3.893 \cdot 10^{-3} \text{ m}^2$ |
| Hydraulic diameter                                  | $1.347 \cdot 10^{-2} \text{ m}$   |
| Spacer grid $K_{loss}$                              | 1.68                              |
| Total heat transfer area of the heated part of rods | $3.2928 \text{ m}^2$              |
| Maximum linear heat rate                            | 2.441 kW/m                        |

**Figure 2. CATHARE model of the FEBA rod bundle.**

### 3.3. Base calculation of FEBA test 216

The reflood transient begins when the experimental initial clad temperature at 1625 mm is reached. By starting of the test run the bundle power was increased to the required level simulating decay heat according to 120% ANS-Standard about 40 s after reactor shut down. Simultaneously the water supply was activated. The initial and boundary conditions (BIC) of FEBA test 216 are shown in Table 2.

**Table 2. Initial and boundary conditions of FEBA test 216**

| Test | Power Law | Pressure [bar] | Reflood rate [cm/s] | Flooding Temperature (begin / end) [C] | Assembly power [KW] |
|------|-----------|----------------|---------------------|--|---------------------|
| 216  | 120% ANS  | 4.1            | 3.8                 | 63 / 37                                | 200                 |

The results of base calculation of test 216 are shown in Fig. 3 and Fig. 4. CATHARE2 calculation underestimates the cladding temperature at FEBA level 1680 mm (where the exp. PCT is located) and predicts faster quench front propagation comparing to the experimental data. Quenching is simulated by the code with activated bottom-top (BT) and top-bottom (TB) reflood models. No top-bottom quench is shown on Fig. 4. Similar results were obtained by CEA, Bel V and ISRN that have used CATHARE2 V2.5\_2 mod 8.1 in the framework of PREMIUM benchmark [6]. The detailed comparison of the results together with accuracy quantification based on Fast Fourier Transformation is provided in Section 5.1.

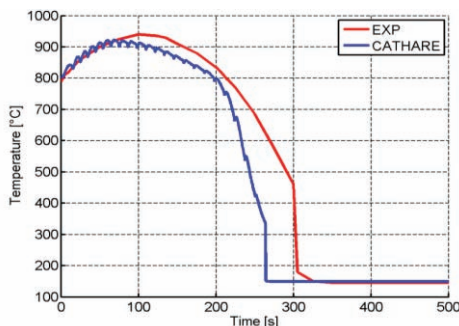


**Figure 3. Calculated and measured wall temperatures at 1680 mm (FEBA 216).**

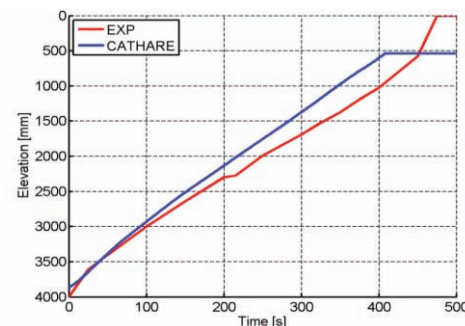


**Figure 4. Quench front propagation (FEBA 216).**

Intensive sensitivity studies of the FEBA model have been performed based on test 216. The following cases were studied:

- Effect of axial nodalization scheme. The number of axial meshes was decreased from 39 to 27. Based on the obtained results it was concluded that the influence of the axial nodalization is rather small;
- Effect of axial pressure loss coefficient. The axial singular pressure loss coefficient was set to  $K_{loss} = 0$  and  $K_{loss} = 10.0$ . The higher pressure loss coefficient ( $K_{loss} = 10.0$ ) leads to a slightly earlier quenching and insignificantly smaller clad temperature. This difference was considered rather as negligible with respect to the accuracy of calculation results;
- Effect of activation of the TOP-BOTTOM reflood. No significant difference was observed in the calculation results. The top-bottom reflood weakly affects the bottom-top quench motion;
- Effect of the rod simulator material properties. The corresponding specific heat capacities of FEBA materials (MgO, NiCr and V2A steel) were varied by +/-5%. The effect of such variation is significantly less than the effect of wall-to-fluid global heat transfer, conduction near quench front and interfacial friction [7]. Furthermore, the effect of FEBA materials thermal conductivity was studied by changing the corresponding values by +/-5%. Differences in results prediction due to this

variation may be considered rather as negligible. At the end, the influence of material density was investigated by varying its values by +/- 5%. The effect of such variation is comparable to the impact of specific heat capacity. Overall, the biggest influence on the prediction results has the variation of MgO properties, however is much less than the effect of bias in the interfacial friction or heat exchange model downstream the quench front. Similar conclusions about the influence of material properties on the CATHARE2 predictions were drawn by the CEA in Phase-II of the PREMIUM benchmark [6];

- Effect of reflood dynamic mesh. In order to assess the effect of reflood dynamic mesh, calculation of the FEBA test 216 test with two different types of the dynamic meshes has been performed. In Table 3 and Table 4 is shown distribution of length (in [m]) of the correspondent reflood meshes. Generally, the calculations do not exhibit any significant change. The dynamic mesh of Type 1 was considered as the reference in all the FEBA tests calculations.

**Table 3. Dynamic reflood mesh Type 1**

|          |          |          |          |          |
|----------|----------|----------|----------|----------|
| 1,00E-02 | 8,15E-03 | 8,00E-03 | 8,00E-03 | 5,00E-03 |
| 5,00E-03 | 1,00E-03 | 1,00E-03 | 5,00E-04 | 5,00E-04 |
| 5,00E-04 | 5,00E-04 | 5,00E-04 | 5,00E-04 | 5,00E-04 |
| 2,00E-04 | 1,00E-04 | 1,00E-04 | 1,00E-04 | 2,00E-04 |
| 5,00E-04 | 5,00E-04 | 5,00E-04 | 5,00E-04 | 5,00E-04 |
| 5,00E-04 | 5,00E-04 | 1,00E-03 | 1,00E-03 | 5,00E-03 |
| 5,00E-03 | 8,00E-03 | 8,00E-03 | 8,15E-03 | 1,00E-02 |

**Table 4. Dynamic reflood mesh Type 2**

|          |          |          |          |          |
|----------|----------|----------|----------|----------|
| 2,50E-02 | 1,00E-02 | 4,00E-03 | 1,00E-03 | 5,00E-04 |
| 2,00E-04 | 1,00E-04 | 4,00E-05 | 1,00E-04 | 2,00E-04 |
| 5,00E-04 | 5,00E-04 | 5,00E-04 | 5,00E-04 | 9,00E-04 |
| 1,00E-03 | 1,00E-03 | 1,00E-03 | 1,00E-03 | 1,00E-03 |
| 1,00E-03 | 1,00E-03 | 1,00E-03 | 1,00E-03 | 1,00E-03 |
| 1,00E-03 | 5,00E-03 | 5,00E-03 | 5,00E-03 | 5,00E-03 |
| 5,00E-03 | 5,00E-03 | 5,00E-03 | 5,00E-03 | 5,00E-03 |

### 3.4. Calculation of FEBA test 214

The reference nodalization of FEBA test section was used to simulate FEBA test 214. The BIC of FEBA test 214 is shown in Table 5. Results of the calculation are shown in Fig. 5 and Fig. 6. CATHARE2 calculation underestimates the clad temperature at FEBA level 1680 mm (where the exp. PCT is located) and predicts faster quench front propagation comparing to the experimental data. The detailed comparison of the results accompanied by accuracy quantification based on Fast Fourier Transformation is provided in Section 5.1.

**Table 5. Initial and boundary conditions of FEBA test 214**

| Test | Power Law | Pressure [bar] | Reflood rate [cm/s] | Flooding Temperature (begin / end) [C] | Assembly power [kW] |
|------|-----------|----------------|---------------------|--|---------------------|
| 214  | 120% ANS  | 4.1            | 5.8                 | 45 / 37                                | 200                 |

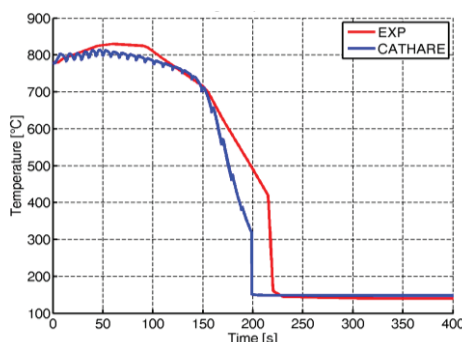


**Figure 5. Calculated and measured wall temperatures at 1680 mm (FEBA 214).**

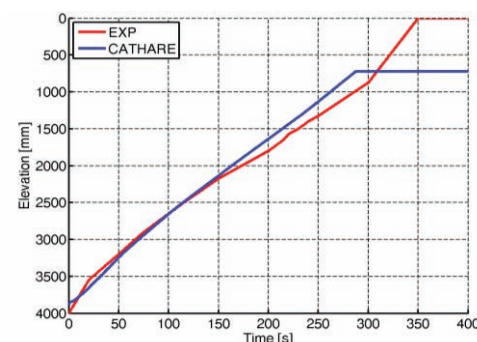


**Figure 6. Quench front propagation (FEBA 214).**

## 4. VALIDATION OF CATHARE AGAINST ACHILLES REFLOODING EXPERIMENTS

### 4.1. Description of ACHILLES test facility

The ACHILLES test facility [8] was designed to investigate the heat transfer in the core of a PWR during the reflood phase of a postulated large break loss of coolant accident. The ACHILLES test section consisted of 69 fuel rod simulators, assembled into a cluster using spacer grids, and mounted vertically within a cylindrical shroud vessel. Each fuel rod simulator had the same heated length as a PWR fuel rod (3.66 m) and the same diameter (9.5 mm). A cross-sectional diagram of the cluster and shroud vessel, the axial power distribution, the location of spacer grids and instrumentation positions are shown in Fig. 7.

### 4.2. Modeling of ACHILLES facility with 1-D approach

The same modelling approach has been used for the simulation of the ACHILLES facility as adopted previously for the calculation of the FEBA test: single 1-D hydraulic channel representing the test section with 1 heat structure component reproducing the entire fuel bundle and the other one representing the cylindrical shroud (Fig. 8). The axial element is of the type “rod bundle” with 28 axial segments. Only the heated part of the test section is modeled. The nodalization features are summarized in Table 6.

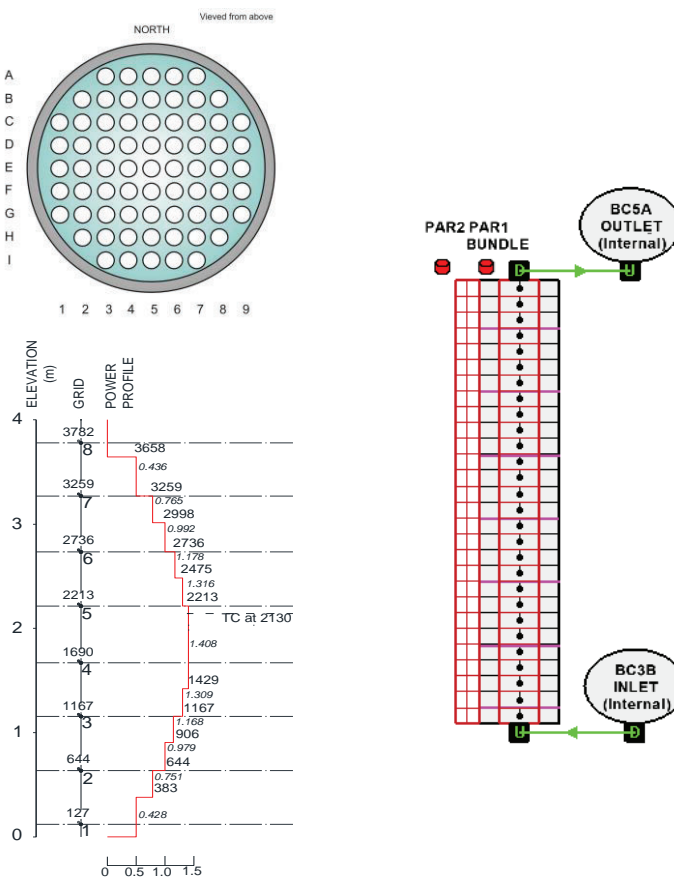


**Figure 7. ACHILLES rod bundle – cross-section view and axial power profile distribution.**

**Figure 8. CATHARE model of the ACHILLES rod bundle.**

**Table 6. Summary of CATHARE2 model of ACHILLES facility**

| Parameter  | Value                             |
|--|-----------------------------------|
| Total height/length  | 3.658 m                           |
| Node in heated length                                      | 28                                |
| Flow area  | $7,977 \cdot 10^{-3} \text{ m}^2$ |
| Hydraulic diameter   | $1,296 \cdot 10^{-2} \text{ m}$   |
| Spacer grid $K_{loss}$                                     | 1.2                               |
| Total heat transfer area of the heated part of heater rods | 7.53 $\text{m}^2$                 |
| Maximum linear heat rate                                   | 1.15 $\text{kW/m}$                |

The 7 grid spacers are modeled according to the specifications. However, no change in hydraulic diameter or flow area reduction is modeled at the spacer grids elevations. The thick-wall housing is modelled (thickness is 6.5 mm), whereas unheated part of rods, lower and upper plenum are not modeled. Thermal properties of the materials are obtained by a linear or a polynomial regression from ACHILLES data [8].

Intensive sensitivity studies of the ACHILLES 1-D model have been performed using the base case test A1R030 (Table 7). The same strategy to the one implemented in case of FEBA was utilized to study the effect of axial nodalization, the effect of axial pressure loss coefficient, the effect of TOP-BOTTOM reflood and the effect of reflood dynamic mesh on calculation results. It should be noted that majority of these sensitivity studies do not exhibit any relevant difference between the calculation results. The relative attention should be paid while choosing the noding of dynamic reflood mesh, since it may affect the timing of reflood process (~ 5-10%). However, sensitivity study on the reflood dynamic mesh in case of FEBA test 216 does not shows any significant difference between the calculation results.

In order to reach the Start of Transient conditions, no steady state calculation was performed but a set-up of the cladding and shroud vessel temperatures. As to the initial conditions, all junction flow was set to stagnation, while the steam temperature was set to the value slightly above the saturation (200°C).

#### **4.3. Calculation and analysis of ACHILLES tests using 1-D CATHARE models**

Several tests were selected for code assessment, covering a wide range of operation parameters: system pressure, water inlet mass flow rate, water inlet flow subcooling and heat flux. In the current studies, calculations of the ACHILLES tests A1R028, A1R030, A1R045, A1R047 and A1R048 using CATHARE2 v2.5\_2 mod 7.1, v2.5\_3 mod 3.1 and CATHARE3\_v1.3.13 have been performed. Initial and boundary conditions of these tests are presented in Table 7.

**Table 7. Initial and boundary conditions of the selected ACHILLES tests**

| Test   | Description             | Pressure<br>[bar] | Reflood rate<br>[cm/s] | Inlet subcooling<br>[C] | Rod power<br>[kW] |
|--------|-------------------------|-------------------|------------------------|-------------------------|-------------------|
| A1R030 | Base case: 70% ANS + 2σ | 2.1               | 2.0                    | 24                      | 3.0               |
| A1R028 | High constant power     | 2.1               | 2.0                    | 22                      | 2.5               |
| A1R045 | High pressure           | 4.1               | 2.0                    | 23                      | 3.0               |
| A1R047 | High subcooling         | 2.1               | 2.0                    | 53                      | 3.0               |
| A1R048 | High flow               | 2.1               | 4.0                    | 24                      | 3.0               |

##### **4.3.1. Assessment of the CATHARE2 and CATHARE3 two-fluid six-equation models [1-D]**

The ACHILLES test A1R030 was selected as base case to assess the reference model and to perform sensitivity studies. The reference set-up is unique for all of the selected CATHARE versions and modes and it uses the dynamic reflood mesh of Type 2 (Table 4).

The results of calculation of ACHILLES test A1R030 are shown in Fig. 9 and Fig. 10. Quenching is simulated by the codes with activated bottom-top (BT) and top-bottom (TB) reflood models. No top-bottom quench is shown on Fig. 10. The cladding temperature calculated by codes is closer to the experimental temperature of external heater rods (G7, H8). In Fig. 10 can be seen that CATHARE3 two-field calculation exhibits faster quench front propagation in comparison to the results by CATHARE2 V2.5\_2 and V2.5\_3. As a consequence, the peak wall temperatures calculated by CATHARE3 are slightly below (~ 50°C) of the temperatures that are calculated by CATHARE2. However, no difference in results prediction is observed in case of CATHARE2 V2.5\_2 and V2.5\_3.

The experimental quench front propagation at the top of fuel assembly is influenced by a top-down reflood caused by liquid fall-back from the separation devices installed above test section. These components were not modeled and, therefore, the top-down reflood phenomenon was not modeled to full extent. Nonetheless, this does not affect the bottom-top quench front propagation for the major part of the assembly and, therefore, the discrepancies between predicted quench front elevation and experimental data at the top of fuel assembly may be neglected. It should be also noted that calculations have been performed as “post-test”, i.e. experimental results were available to the analyst. However, no special tuning has been applied to the models in order to achieve best agreement possible with experimental data.

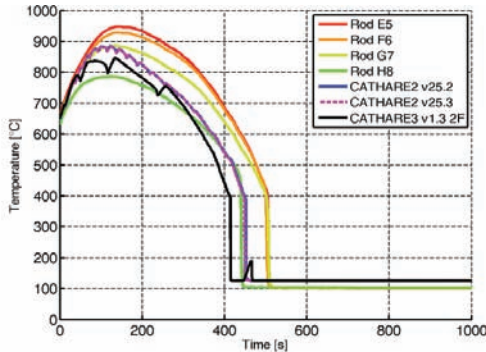


**Figure 9. Calculated and measured wall temperatures at 2130 mm (A1R030).**

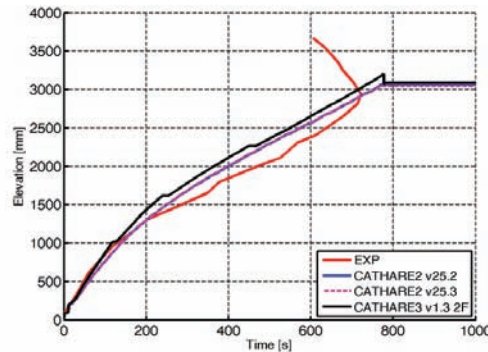


**Figure 10. Quench front propagation (A1R030).**

All the selected tests (A1R028, A1R045, A1R047 and A1R048) show similar wall temperature behavior and the quench front propagation as to the base run A1R030. The detailed comparison of the results accompanied by accuracy quantification based on Fast Fourier Transformation is provided in Section 5.2.

#### 4.3.2. Assessment of the CATHARE3 three-field model [1-D]

The Fig. 11 and Fig. 12 show the effect of activation of the droplet field on quenching in ACHILLES test A1R030. Basically, it results in much faster quench front propagation in comparison to the experimental trend and to the one obtained by two-fluid six-equation CATHARE3 model.

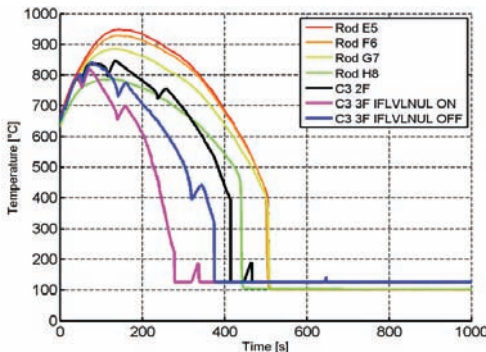


**Figure 11. Calculated and measured wall temperatures at 2130 mm (A1R030).**

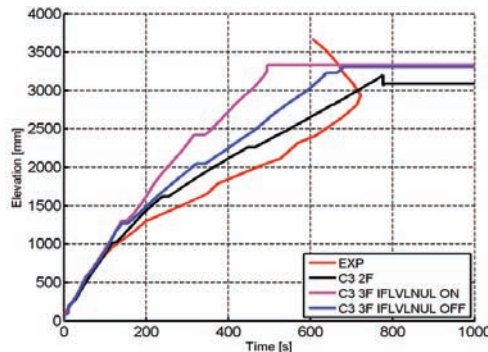


**Figure 12. Quench front propagation (A1R030).**

Besides, it was discovered a strong effect of IFLVLNUL flag on code prediction (Fig. 11 and Fig. 12). This flag affects the behavior of vanishing liquid film downstream the quench front. By default settings, in CATHARE3 is used IFLVLNUL ON [9], that means that velocity of vanishing continuous liquid film is set to zero ( $V_{\text{liquid}} = 0$ ). From the other side, flag IFLVLNUL OFF sets velocity of vanishing liquid film to the velocity of gas ( $V_{\text{liquid}} = V_{\text{gas}}$ ). Consequently, the wall friction and the interfacial friction are not corrected in this case to take into account the fact that the liquid film velocity is close to zero.

It should be noted that reference CATHARE3 model with activated droplet field uses IFLVLNUL flag OFF. Further results analysis together with accuracy quantification is provided in Section 5.2.

#### 4.4. Modeling of ACHILLES facility with 3-D features of CATHARE2

In order to assess the performance of the 3-D reflood model implemented in CATHARE2, a three-dimensional thermal-hydraulic nodalization of the experimental bundle was developed using one rectangular 3-D module (Fig. 13 and Fig. 14). Only the heated part of the test section is modeled. The 3-D component has a dimension of  $5 \times 5 \times 28$  meshes. Boundary conditions are applied to the inlet and outlet of the volume elements that are connecting all the hydraulic channels upstream and downstream.

The 69 fuel rod simulators are represented by a 25 heat structures (1 internal heat structure per 1 hydraulic channel). Thus, the 25 reflood elements (REFLCH3D) are used in the simulation. The dynamic reflood mesh that is utilized in the 3-D model is the same to the one that was used in case of ACHILLES 1-D model with 28 axial meshes. The thick-wall housing is modelled by 16 external walls that are located at the periphery of the test assembly.

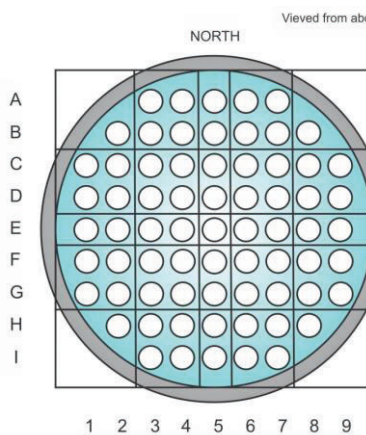


**Figure 13. Radial meshing of the ACHILLES bundle.**

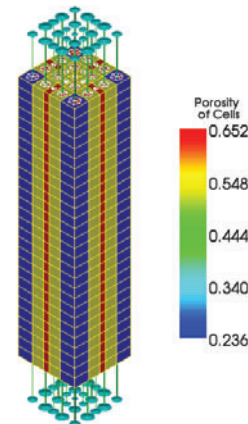


**Figure 14. 3-D nodalization layout of the ACHILLES (with porosity of the channels).**

In order to simulate the pressure loss due to flow restriction, the 7 grid spacers are modeled according to the specifications. To account the influence of the rods on the transversal flow, it was used a transversal singular pressure loss coefficient calculated with Idel'chik formulation [10] and corrected by the ratio of the flow areas in CATHARE and Idel'chik representation [11, 12].

The results of calculation of the ACHILLES test A1R030 are shown in Fig.15 and Fig. 16. Quenching is simulated by the code with activated bottom-top reflood. Calculation of the test with reference CATHARE2 3-D model underpredicts by  $\sim 50^{\circ}\text{C}$  the temperature of cladding at 2130 mm in the central fuel rod (rod E5, where the exp. PCT is located). On the other hand, the wall temperature at the peripheral

rod H8 is slightly overpredicted at the beginning of the reflood test (at the time  $\sim 50$ s). In Fig.16 can be seen that the calculated quenching front is slightly faster than the experimental one.

Generally it can be noticed, that the results calculated by 1-D and 3-D CATHARE models are in the fair agreement between each other. The three-dimensional approach allows obtaining of the cladding temperature distribution in the test bundle, whereas calculation by one-dimensional model provides the value averaged over test section. The detailed comparison of the results obtained by CATHARE2 3-D model for the selected ACHILLES tests is provided in Section 5.2.

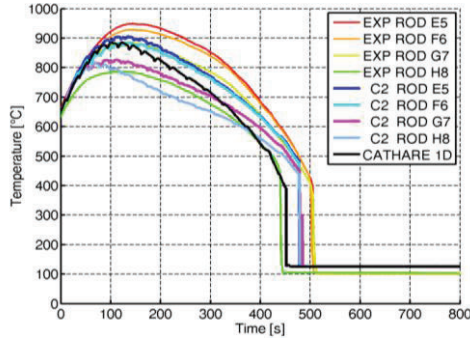


**Figure 15. Calculated and measured wall temperatures at 2130 mm (A1R030).**

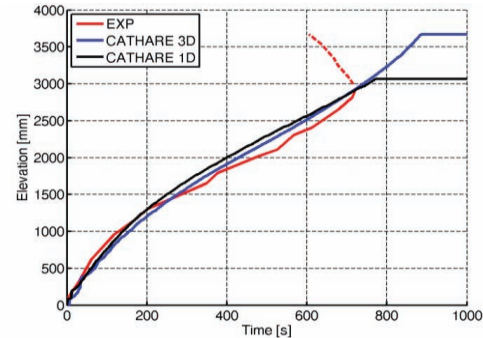


**Figure 16. Quench front propagation (A1R030).**

## 5. ACCURACY QUANTIFICATION

Quantification of the accuracy of code calculations is performed using the Fast Fourier Transform Based Method (FFTBM), that has been originally developed to quantify the accuracy of a given code calculation [13]. With FFTBM the quantification of the accuracy of code calculations is performed using amplitude of the Fourier Transform of the experimental signal and of the difference between this one and the calculated trend. Therefore, the comparison between experimental data and calculation results is performed in frequency domain, eliminating the dependence of the method on time duration of experiment and shape of analyzed time trends. The FFTBM tool itself has been validated and applied in the numerous international benchmarks [14].

### 5.1. FEBA tests

The following parameters have been selected as responses from available set of measurements:

- Cladding temperature at location 12b4 (where the exp. PCT is observed, 1680 mm);
- Cladding temperature at location 12b2 (top of active fuel, 590 mm);
- Quench front elevation (QF).

These 3 responses represent at best the relevant issues of reflood in nuclear safety: PCT and the time of core quench. Weights  $w_z$  of the corresponding responses were determined as it is described in [15] and are presented in Table 8.

It should be noticed that the time sampling ranges (Table 9) were applied during the accuracy quantification step in order to evaluate more thoroughly the capabilities of CATHARE models to predict wall temperatures around its maximum value.

The results of accuracy quantification (i.e. Global Average Amplitude value) for FEBA test 214 and 216 are shown in Table 10. The lower is the AAGlobal – the better is agreement between the experiment and calculation. Comparison of the absolute values of experimental (Exp) and calculated (Calc) peak cladding temperature and quenching time, as well as corresponding relative differences ( $\Delta_{Rel} = \frac{Exp - Calc}{Exp}$ ) is provided in Table 11.

**Table 8. Calculated weights of the responses**

| Parameter    | Value $w_z$ |
|--------------|-------------|
| Tclad 12b4   | 0.357       |
| Tclad 12b2   | 0.357       |
| Quench front | 0.286       |

**Table 9. Time sampling ranges for FEBA test 214 and 216**

| FEBA test | T12b2                  |                        | T12b4                  |                        | QF                     |                        |
|-----------|------------------------|------------------------|------------------------|------------------------|------------------------|------------------------|
|           | T <sub>min</sub> , [s] | T <sub>max</sub> , [s] | T <sub>min</sub> , [s] | T <sub>max</sub> , [s] | T <sub>min</sub> , [s] | T <sub>max</sub> , [s] |
| 214       | 0.0                    | 250.0                  | 0.0                    | 190.0                  | 0.0                    | 300.0                  |
| 216       | 0.0                    | 350.0                  | 0.0                    | 220.0                  | 0.0                    | 400.0                  |

From the results can be seen that CATHARE2 underestimates the peak cladding temperature (~3-4%) and predicts faster quench front propagation comparing to experimental data (~10%). The difference of few percent in the PCT prediction for both of FEBA tests is rather good result comparing to the uncertainty of the calculations [7].

**Table 10. Calculated Global Average Amplitude for FEBA test 214 and 216**

| FEBA test | AAGlobal |
|-----------|----------|
| 214       | 0.178    |
| 216       | 0.183    |

**Table 11. Comparison of PCTs and quenching times**

| FEBA test | Quantity    | EXP | Calc | $\Delta_{Rel}[\%]$ |
|-----------|-------------|-----|------|--------------------|
| 214       | PCT, [°C]   | 830 | 805  | -3.0%              |
|           | Q_time, [s] | 310 | 270  | -12.9%             |
| 216       | PCT [°C]    | 940 | 920  | -4.2%              |
|           | Q_time, [s] | 450 | 410  | -9.7%              |

## 5.2. ACHILLES tests

The following parameters have been selected as responses from available set of measurements:

- Cladding temperature at location 2130 mm, rod E5 (T<sub>2\_130</sub>, where the exp. PCT is observed);
- Cladding temperature at location 2423 mm, rod F5 (T<sub>2\_423</sub>);
- Quench front elevation (QF).

The weights  $w_z$  of the aforementioned responses correspond to the ones that were used for accuracy quantification of the FEBA tests 214 and 216 (Table 8). The time sampling ranges (Table 12) were applied for accuracy quantification. The results of accuracy quantification (i.e. AAGlobal) for ACHILLES tests calculated with CATHARE2 V2.5\_2 mod 7.1 (1-D), V2.5\_3 mod 3.1 (1-D and 3-D), CATHARE3 two-field (1-D), CATHARE3\_v1.3 three-field (1-D) are presented in Table 13. Comparison of the absolute values of experimental (Exp) and calculated (Calc) peak cladding temperature (PCT) and quenching time (Q\_time), as well as corresponding relative differences is provided in Table 14.

**Table 12. Time sampling ranges for selected ACHILLES tests**

| ACHILLES test | T2_130                 |                        | T2_423                 |                        | QF                     |                        |
|---------------|------------------------|------------------------|------------------------|------------------------|------------------------|------------------------|
|               | T <sub>min</sub> , [s] | T <sub>max</sub> , [s] | T <sub>min</sub> , [s] | T <sub>max</sub> , [s] | T <sub>min</sub> , [s] | T <sub>max</sub> , [s] |
| A1R028        | 0.0                    | 400.0                  | 0.0                    | 500.0                  | 0.0                    | 999.0                  |
| A1R030        | 0.0                    | 400.0                  | 0.0                    | 500.0                  | 0.0                    | 700.0                  |
| A1R045        | 0.0                    | 250.0                  | 0.0                    | 350.0                  | 0.0                    | 450.0                  |
| A1R047        | 0.0                    | 380.0                  | 0.0                    | 450.0                  | 0.0                    | 620.0                  |
| A1R048        | 0.0                    | 300.0                  | 0.0                    | 350.0                  | 0.0                    | 420.0                  |

**Table 13. Calculated Global Average Amplitude for selected ACHILLES tests**

| ACHILLES test | AAGlobal  |           |                    |                    |           | 3-D |  |
|---------------|-----------|-----------|--------------------|--------------------|-----------|-----|--|
|               | 1-D       |           |                    |                    |           |     |  |
|               | C2 V2.5_2 | C2 V2.5_3 | C3 V1.3.13 2-field | C3 V1.3.13 3-field | C2 V2.5_3 |     |  |
| A1R028        | 0.208     | 0.208     | 0.275              | 0.991              | 0.134     |     |  |
| A1R030        | 0.208     | 0.210     | 0.323              | 0.992              | 0.112     |     |  |
| A1R045        | 0.190     | 0.192     | 0.494              | 0.870              | 0.087     |     |  |
| A1R047        | 0.273     | 0.286     | 0.420              | 1.026              | 0.101     |     |  |
| A1R048        | 0.370     | 0.380     | 0.659              | 0.883              | 0.095     |     |  |

**Table 14. Comparison of PCTs and quenching times**

| ACHILLES test | Quantity    | Exp | 1-D       |                |           |                |            |                | 3-D        |                |           |
|---------------|-------------|-----|-----------|----------------|-----------|----------------|------------|----------------|------------|----------------|-----------|
|               |             |     | C2 V2.5_2 |                | C2 V2.5_3 |                | C3 V1.3.13 |                | C3 V1.3.13 |                | C2 V2.5_3 |
|               |             |     | Calc      | $\Delta_{Rel}$ | Calc      | $\Delta_{Rel}$ | Calc       | $\Delta_{Rel}$ | Calc       | $\Delta_{Rel}$ | Calc      |
| A1R028        | PCT, [°C]   | 945 | 870       | -7,9           | 870       | -7,9           | 825        | -12,7          | 808        | -14,5          | 900       |
|               | Q_time, [s] | 100 | 1000      | 0,0            | 1000      | 0,0            | 970        | -3,0           | 825        | -17,5          | 930       |
| A1R030        | PCT, [°C]   | 950 | 890       | -6,3           | 891       | -6,2           | 849        | -10,6          | 845        | -11,1          | 905       |
|               | Q_time, [s] | 720 | 770       | 6,9            | 766       | 6,4            | 771        | 7,1            | 680        | -5,6           | 875       |
| A1R045        | PCT, [°C]   | 920 | 914       | -0,7           | 914       | -0,7           | 875        | -4,9           | 869        | -5,5           | 920       |
|               | Q_time, [s] | 495 | 480       | -3,0           | 481       | -2,8           | 468        | -5,5           | 410        | -17,2          | 581       |
| A1R047        | PCT, [°C]   | 972 | 902       | -7,2           | 902       | -7,2           | 868        | -10,7          | 862        | -11,3          | 920       |
|               | Q_time, [s] | 640 | 681       | 6,4            | 679       | 6,1            | 701        | 9,5            | 600        | -6,3           | 835       |
| A1R048        | PCT, [°C]   | 785 | 711       | -9,4           | 710       | -9,6           | 705        | -10,2          | 700        | -10,8          | 740       |
|               | Q_time, [s] | 520 | 450       | -13,5          | 453       | -12,9          | 442        | -15,0          | 302        | -41,9          | 598       |

General comparison of the measured and calculated PCTs for the selected ACHILLES tests is shown on Fig. 17. It can be seen that the best agreement with experiment is achieved in case of CATHARE2 V2.5\_3 mod 3.1 [3-D] modelling approach. The discrepancy between the code prediction and experimental data is smaller in case of the test at high pressure (i.e. test A1R048, see Fig. 17). Instead, the largest differences are encountered in case of the test A1R028 that is conducted at high constant power.

All the temperatures calculated with CATHARE2 (both 1-D and 3-D) fits the uncertainty margin +/- 10%, that is corresponding to the discrepancy of ~100 °C in the PCT prediction. CATHARE2 v2.5\_3 mod 3.1 shows mainly the same results as CATHARE2 v2.5\_2 mod 7.1. It can be noticed that the accuracy of the results (i.e. AAGlobal) obtained by CATHARE3 v1.3 two-field is smaller in average by ~ 0.18 from those obtained by CATHARE2 V2.5\_3 mod 3.1 Table (based on Table 13).

The biggest discrepancy between the prediction and measurements is exhibited in case of CATHARE3 v1.3.13 with activated three-field model. In this case the presence of the droplet field improves the heat transfer in the bundle by accounting the liquid droplets entrainment from the near-wall liquid film and

consequently increases the velocity of the quench front propagation. As a result, the peak cladding temperature is underpredicted by CATHARE3 three-field model in all of the selected test cases.

In case of ACHILLES test A1R048 (high mass flow, Table 7), the difference in PCT calculated by the three-field model and the six-equation model is the smallest among the considered tests. It may be explained by the fact that the velocity of liquid film in the annular flow downstream the quench front tends to the velocity of droplets and so the effect of the droplet field becomes smaller. Indeed, with increase of the difference between the velocity of near-wall continuous liquid and the velocity of liquid droplets, the importance of the third field modeling is rising.

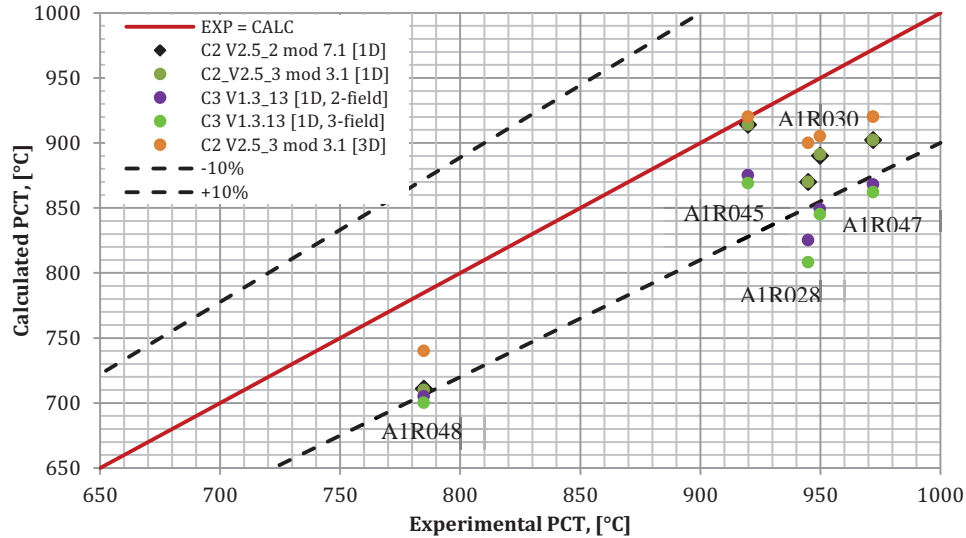


**Figure 17. Calculated PCT versus measured PCT (ACHILLES).**

## 6. CONCLUSIONS

The present paper shows the validation activity that has been carried to assess CATHARE2 V2.5\_3 mod 3.1 code capabilities to simulate scenarios featuring reflood conditions. For such purpose, selected experiments have been simulated using 1-D model in case of FEBA test facility and both 1-D/3-D models in case of ACHILLES. Furthermore, the capabilities of the new CATHARE3 v1.3.13 code to simulate reflood phenomena using both six-equation and three-field one-dimensional models has been assessed, based on the same ACHILLES tests.

An intensive sensitivity studies have been performed for each of the experimental test facilities in order to set-up a reference calculation model. Quantitative analysis of the results has been carried out for all of the considered tests, using the Fast Fourier Transform Based Method (FFTBM) for accuracy quantification of code predictions. The major conclusions from the performed validation work are drawn below:

1. Most CATHARE2 simulations of reflood tests predict an earlier quenching time compared to the measured data. The reasons for such behavior may be the systematic code underprediction of the interfacial friction and overprediction of the wall to fluid heat transfer coefficient in the annular flow (or annular-mist) downstream the quench front;
2. The no-regression of the results predicted by CATHARE2 V2.5\_3 mod 3.1 was successfully checked through qualitative and quantitative comparison with results obtained by one of the previous code versions: CATHARE2 v2.5\_2 mod 7.1;

3. In majority of the selected ACHILLES test cases, CATHARE3\_v1.3.13 (two-field) shows relatively close results to the CATHARE2 but with slightly earlier quenching;
4. Application of CATHARE3 v1.3.13 (three-field) to the ACHILLES tests shows a considerable difference from CATHARE2 predictions, mainly because of the significantly faster quenching. It may be explained by the presence of the droplet field that improves the heat transfer in the bundle by accounting for the liquid droplets entrainment from the near-wall liquid film and consequently increasing the velocity of the quench front propagation. Further investigation on such behavior is needed;
5. The three-dimensional model of ACHILLES test facility has been developed and assessed using CATHARE2 v2.5\_3 mod 3.1. Based on the results of quantitative analysis (FFTB), the best agreement with experiment among the tested models is achieved using the 3-D model.

## ACKNOWLEDGMENTS

This work has been performed in the framework of the NURESAFE European collaborative project, financially supported by European Commission.

## REFERENCES

1. G. Lavialle, *CATHARE 2 V2.5\_3mod3.1 code: General description*, DEN/DANS/DM2S/STMF/LMES/NT/1 3-017/A (2013).
2. P. Emonot, A. Souyri, J.L. Gandrille, F. Barré, “CATHARE-3: A new system code for thermal-hydraulics in the context of the NEPTUNE project,” *Proceedings of NURETH 13 conference* (2009).
3. A.Guelfi et. al., “NEPTUNE A new Software Platform for advanced Reactor Thermalhydraulics,” *Nucl. Sc. and Eng.*, **156**, pp.282-324 (2007).
4. F. Barré, M. Parent, B. Brun, “Advanced numerical methods for thermal hydraulics,” *Nucl. Eng. Des.*, **145**, pp.147-158 (1993).
5. KfK Karlsruhe, *FEBA – Flooding Experiments with Blocked Arrays*, KfK 3657 (1984).
6. NEA-CSNI, *Post-BEMUSE Reflood Model Input Uncertainty Methods (PREMIUM) Benchmark Phase II: Identification of Influential Parameters*, Tech. Rep., Committee on the Safety of Nuclear Installations, OECD, Nuclear Energy Agency (2015).
7. A. Kovtonyuk, S. Lutsanych, F. Moretti and A. Petrucci, “Development and assessment of a method for evaluating uncertainty of input parameters,” *Proceedings of NURETH-16 conference (submitted for publication)* (2015).
8. ACHILLES, “Achilles Unballooned Cluster Experiments - Part 1: Description of the Achilles Rig, Test Section and Experimental Procedures,” *Tech. Rep. AEEW-R 2336*, United Kingdom Atomic Energy Authority, Winfrith Technology Centre (1989).
9. *CATHARE3\_v1\_3.2 code: Dictionary of operators and directives*, DEN/DANS/DM2S/STMF/EQUIPE CATHARE3 (2014).
10. I. E. Idel'chik, *Handbook of Hydraulic Resistance*, Begell House, ISBN-10: 1567000746, (2001).
11. G. Serre, D. Bestion, *Benchmarks calculated with the ICE numerical method using CATHARE and TRIO-U codes*, DEN/DTP/SMTH/LMDS (2001).
12. S. Lutsanych, L. Sabotinov, F. D'Auria, “Critical Power Prediction by CATHARE2 of the OECD/NRC BFBT Benchmark,” *Nucl. Eng. Des.*, DOI: 10.1016/j.nucengdes.2014.06.038, (2014).
13. W. Ambrosini, R. Bovalini, F. D'Auria, “Evaluation of Accuracy of Thermal-hydraulic Codes Calculations,” *Energia Nucleare* 7 (1990).
14. A. Petrucci and F. D'Auria, “Uncertainties in Predictions by Thermal-Hydraulic Codes: Approaches and Results,” *8th Int. Conference on Nanochannels, Microchannels and Minichannels* (2010).
15. A. Kovtonyuk, *PhD Thesis: Development of methodology for evaluation of uncertainties of system thermal-hydraulic codes' input parameters*, <https://etd.adm.unipi.it/etd-05082014-001322/>, pp. 30-34, University of Pisa, 2014.